Inorganic Chemistry

Article

pubs.acs.org/IC

Dissociation of Diglycolamide Complexes of Ln^{3+} (Ln = La–Lu) and An^{3+} (An = Pu, Am, Cm): Redox Chemistry of 4f and 5f Elements in the Gas Phase Parallels Solution Behavior

Yu Gong, Guoxin Tian, Linfeng Rao, and John K. Gibson*

Chemical Sciences Division, Lawrence Berkeley National Laboratory, Berkeley, California 94720, United States

Supporting Information

ABSTRACT: Tripositive lanthanide and actinide ions, Ln^{3+} (Ln = La–Lu) and An^{3+} (An = Pu, Am, Cm), were transferred from solution to gas by electrospray ionization as $Ln(L)_3^{3+}$ and $An(L)_3^{3+}$ complexes, where L = tetramethyl-3-oxa-glutaramide (TMOGA). The fragmentation chemistry of the complexes was examined by collision-induced and electron transfer dissociation (CID and ETD). Protonated TMOGA, HL^+, and $Ln(L)(L–H)^{2+}$ are the major products upon CID of $La(L)_3^{3+}$, $Ce(L)_3^{3+}$, and $Pr(L)_3^{3+}$, while $Ln(L)_2^{3+}$ is increasingly pronounced beyond Pr. A C–O_{ether} bond cleavage product appears upon CID of all $Ln(L)_3^{3+}$; only for $Eu(L)_3^{3+}$ is the divalent complex, $Eu(L)_2^{2+}$, dominant. The CID patterns of $Pu(L)_3^{3+}$, $Am(L)_3^{3+}$, and $Cm(L)_3^{3+}$ are similar to those of the $Ln(L)_3^{3+}$ for the late Ln. A striking exception is the appearance of Pu(IV) products upon CID of $Pu(L)_3^{3+}$, in accord with the relatively low Pu(IV)/Pu(III) reduction potential in solution. Minor divalent $Ln(L)_2^{2+}$ and $An(L)_2^{2+}$ were produced for all Ln and An; with the exception of $Eu(L)_2^{2+}$ these complexes form adducts with O_2, presumably producing superoxides in which the trivalent oxidation state is recovered. ETD of $Ln(L)_3^{3+}$ and $An(L)_3^{3+}$ reveals behavior which parallels that of the Ln^{3+} and An^{3+} ions in solution. A C–O_{ether} bond cleavage product, in which the trivalent oxidation state is preserved, appeared for all complexes; charge reduction products, $Ln(L)_2^{2+}$ and $Ln(L)_3^{2+}$, appear only for Sm, Eu, and Yb, which have stable divalent oxidation states. Both CID and ETD reveal chemistry that reflects the condensed-phase redox behavior of the 4f and 5f elements.

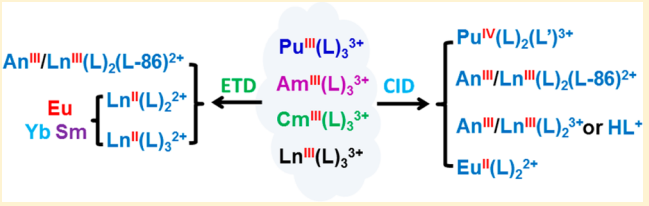

INTRODUCTION

Diglycolamide ligands have been considered as extractants for actinide partitioning due to their high affinities for trivalent lanthanide (Ln) and actinide (An) cations.[1] To understand the behavior of these ligands, a number of studies of their complexation properties in aqueous solutions have been carried out using crystallographic, spectroscopic, and theoretical methods.[2] The extraction behaviors of diglycolamide ligands under different conditions have also been investigated.[2] Knowledge of the stability of diglycolamides toward radiolysis is important for separations processes; in contrast to studies on degradation in solution,[2] only limited information is known about the fragmentation patterns and mechanisms of metal–diglycolamide complexes. Crystalline trivalent lanthanide–diglycolamide complexes have been structurally characterized.[3,4]

It has been demonstrated that gas-phase mass spectrometric studies can be used to probe the fragmentation chemistry of both ligands and ligated complexes absent solvent effects. Collision-induced dissociation (CID) of protonated TMOGA, the most simple diglycolamide ligand (TMOGA = tetramethyl-3-oxa-glutaramide, also referred to as TMDGA, *N,N,N′,N′*-tetramethyl diglycolamide; structure shown in Figure 1), revealed clear relevance to condensed-phase radiolysis.[5] Recently, we investigated the fragmentation chemistry of TMOGA complexes of UO_2^{2+}, NpO_2^{2+}, and PuO_2^{2+}, where

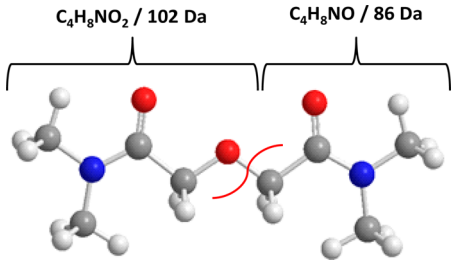

Figure 1. Structure of the TMOGA ligand, $C_8H_{16}N_2O_3$ (mass = 188 Da): red = oxygen; blue = nitrogen; gray = carbon; shaded gray = hydrogen. Fragments produced by C–O_{ether} bond cleavage are identified.

variations in the observed fragmentation patterns and mechanisms reflect the different properties of the three actinyl ions.[6]

Compared with singly and doubly charged cations, it is more difficult to transfer triply charged metal cations from solution to gas phase by electrospray ionization (ESI) due to the absence of the stabilizing effect of the solvent on the high charge state.[7,8] The high third ionization energies of metal ions

Received: August 17, 2014
Published: November 5, 2014

   dx.doi.org/10.1021/ic501985p | Inorg. Chem. 2014, 53, 12135–12140

commonly results in formation of charge-reduction products upon ESI. Recently, stabilization of tetrapositive thorium in the gas phase was achieved via coordination by three tridentate TMOGA ligands;[9] it has been demonstrated that tetrapostive metal ions with the fourth ionization energies up to ~35 eV can be stabilized from solution to gas via ESI by coordination with three TMOGA ligands.[10] It should be relatively facile to stabilize trications under similar conditions. Some transition and lanthanide metal trications coordinated by protic and aprotic ligands have been observed in the gas phase.[11−17] The TMOGA ligand provides an opportunity to understand the chemistry of triply charged complexes of the lanthanide elements as well as of some actinides and to study the same species and charge states as observed in the condensed phase. Furthermore, TMOGA can exhibit C−O bond cleavage to form a bond with the metal center (Figure 1), thereby offering an opportunity to exhibit fragmentation chemistry that depends on the redox properties of the metal center. Reported here is the fragmentation behavior of $Ln(L)_3^{3+}$ for all Ln (except Pm) and $An(L)_3^{3+}$ for An = Pu, Am, and Cm upon CID and electron transfer dissociation (ETD). Upon ETD all complexes fragment in accord with the redox chemistry of the trivalent metal ions in the condensed phase; more diverse chemistry is observed upon CID. Periodic trends across the lanthanide series were observed, and the behaviors of actinide−TMOGA complexes show both similarities and differences compared with the lanthanide complexes.

EXPERIMENTAL DETAILS

All experiments were performed using an Agilent 6340 quadrupole ion trap mass spectrometer (QIT/MS) with the ESI source located inside a radiological containment glovebox.[18] The $Ln(L)_3^{3+}$/$An(L)_3^{3+}$ (Ln = La−Lu; An = Pu, Am, Cm; L = TMOGA) cations were produced by ESI of methanol (<5% water) solutions of TMOGA and either LnX_3 (X = Cl or Br, 200 μM) or $An(ClO_4)_3$ (200 μM for Pu, 10 μM for Am and Cm) with 4:1 excess TMOGA. The actinide isotopes employed were Pu-242, Am-243, and Cm-248, which undergo α-decay with half-lives of 3.7×10^5, 7370, and 3.4×10^5 years, respectively. The MS^n capabilities of the QIT/MS, which designates the ability to perform multiple (n) sequential mass spectrometry stages, allow isolation of ions with a particular mass-to-charge ratio, m/z, followed by CID, in which ions are excited and undergo energetic collisions with helium. The ions isolated inside the trap are at a temperature of around 300 K.[19] ETD was performed using the fluoranthene anion, $C_{16}H_{10}^-$, as the electron donor from which an electron is transferred to a cation. $C_{16}H_{10}^-$ was gated from the negative chemical ionization source into the ion-transfer optics and into the ion trap for reaction with trapped cations. The process associated with introducing anions into the trap may result in incomplete thermalization of the cation complexes in the trap; any such hyperthermal effects should be essentially constant and not appreciably affect comparative results. The ETD reaction time was typically a few milliseconds. In high-resolution mode, the instrument has a detection range of m/z 20−2200 with a mass width (fwhm) of $m/z \approx 0.3$. Mass spectra were recorded in the positive-ion accumulation and detection mode. The intensity distribution of ions in the mass spectra was highly dependent on instrumental parameters, particularly the RF voltage applied to the ion trap; the parameters, similar to those employed in previous experiments,[9,10] are included as Supporting Information. The high-purity nitrogen gas for nebulization and drying in the ion transfer capillary was the boil off from a liquid nitrogen Dewar. As discussed elsewhere,[20,21] the background H_2O and O_2 pressures in the ion trap are estimated to be on the order of 10^{-6} Torr. The helium buffer gas pressure in the trap is constant at $\sim 10^{-4}$ Torr.

RESULTS AND DISCUSSION

ESI of $Ln(L)_3^{3+}$, $Pu(L)_3^{3+}$, $Am(L)_3^{3+}$, and $Cm(L)_3^{3+}$. ESI of LnX_3/TMOGA mixtures in methanol (Figures 2 and S1, Supporting Information) gave similar results for different lanthanides, with $Ln(L)_3^{3+}$ being the predominant species. Assignments of the trication complexes for La, Ce, Pr, Tb, Ho, Tm, and Lu are based on the partially resolved isotopic patterns arising from ^{13}C isotopomers, the first of which is separated by m/z 0.33 from the dominant peak (i.e., $m = 1$ and $z = 3$). The intensities of the first two isotopomer peaks are ca. 26% and 3% relative to that of the dominant fully ^{12}C peak due to the 24 carbon atoms in $Ln(L)_3^{3+}$. Europium has two naturally occurring stable isotopes (^{151}Eu and ^{153}Eu) with similar abundance such that $Eu(L)_3^{3+}$ can be identified on the basis of two peaks with approximately equal intensities separated by m/z 0.67. For the other lanthanides (Nd, Sm, Gd, Dy, Er, Yb), the $Ln(L)_3^{3+}$ complexes exhibit a series of peaks due to the presence of several naturally occurring stable isotopes with comparable abundances; assignment of these $Ln(L)_3^{3+}$ complexes can be made by the m/z 0.33 separation between neighboring peaks. The $Ln(L)_3^{3+}$ assignments were further confirmed by CID and ETD, where dications and monocations were produced as fragmentation products, as discussed below. In addition to the only trication, $Ln(L)_3^{3+}$, dications with compositions $Ln(L)_2X^{2+}$ (X = Cl, Br, OH) were also observed in the ESI mass spectra, albeit at lower intensities. As observed previously,[6,9,10] protonated TMOGA and its fragments as well as impurities such as TMOGA complexes of sodium and calcium cations were also prevalent.

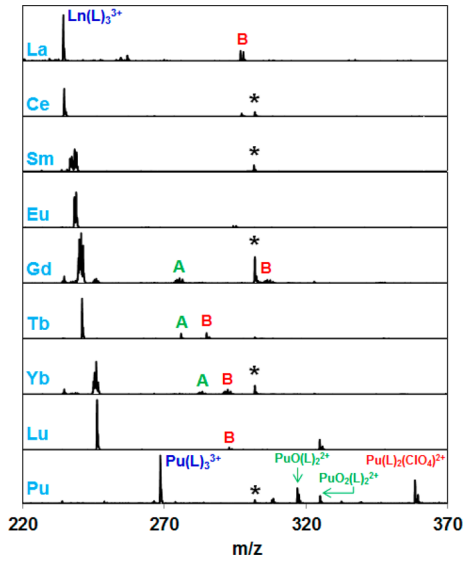

Figure 2. ESI mass spectra of $Pu(ClO_4)_3$/TMOGA as well as of selected LnX_3 (X = Br for La, Ce, Sm and Gd; X = Cl for Eu, Tb, Yb, and Lu) and TMOGA. Asterisks denote the peak due to $Ca(L)_3^{2+}$: (A) $Ln(L)_2(OH)^{2+}$; (B) $Ln(L)_2(X)^{2+}$.

The three actinide trications, $Pu(L)_3^{3+}$, $Am(L)_3^{3+}$, and $Cm(L)_3^{3+}$, were produced by ESI of mixtures of TMOGA and $An(ClO_4)_3$. Identification of these trications is as with lanthanide complexes with a single isotope. In addition to $Pu(L)_3^{3+}$, the ESI mass spectrum of TMOGA and $Pu(ClO_4)_3$ revealed the presence of $Pu^{IV}O(L)_2^{2+}$ and $Pu^{VI}O_2(L)_2^{2+}$, reflecting the stable Pu(IV) and Pu(VI) oxidation states (Figure 2);[22] this contrasts the rather simple spectra for most

dx.doi.org/10.1021/ic501985p | Inorg. Chem. 2014, 53, 12135−12140

$Ln(L)_3^{3+}$ complexes, where Ln(III) is the only common oxidation state. Note that although the Ce(IV) oxidation state is known,[23,24] no detectable Ce(IV) species were observed during ESI of TMOGA and $CeBr_3$, consistent with the fact that the reduction potential for Ce(VI)/Ce(III) (1.70 V) is significantly higher than that for Pu(VI)/Pu(III) (0.98 V).[24] Due to the low concentration of americium and curium used in the experiments, $Am(L)_3^{3+}$ and $Cm(L)_3^{3+}$ were the only detected actinide-containing species in their ESI mass spectra. Both americium and curium have other higher oxidation states but with substantially higher reduction potentials compared with Pu(IV).[22]

CID of $Ln(L)_3^{3+}$, $Pu(L)_3^{3+}$, $Am(L)_3^{3+}$, and $Cm(L)_3^{3+}$. The solid-state structures of some $Ln(L)_3^{3+}$ complexes and analogs have been reported; they exhibit a twisted tricapped trigonal prismatic geometry with the metal center coordinated by nine oxygen atoms.[3,4] It is likely that the gas-phase $Ln(L)_3^{3+}$, $Pu(L)_3^{3+}$, $Am(L)_3^{3+}$, and $Cm(L)_3^{3+}$ complexes have very similar structures to those characterized in the solid state. CID of the lanthanide complexes and the three actinide complexes were performed with spectra for selected $Ln(L)_3^{3+}$ and $An(L)_3^{3+}$ shown in Figures 3, 4, S2, and S3, Supporting Information.

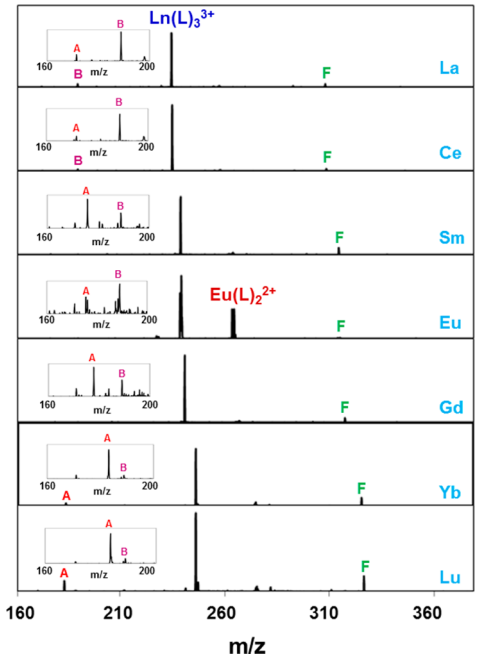

Figure 3. CID mass spectra of selected $Ln(L)_3^{3+}$. A, B, and F denote the peaks due to $Ln(L)_2^{3+}$, HL^+ and $Ln(L)_2(L{-}86)^{2+}$ respectively. Spectra in the m/z 160–200 region are enlarged in the insets. For those Ln having multiple abundant naturally occurring isotopes, Sm, Gd, and Yb in these spectra a single $Ln(L)_3^{3+}$ isotopomer was mass selected for CID.

Although the fragmentation energies are not well established in multiple-collision CID, the CID experiments were performed under the same conditions such that comparison of the relative fragmentation abundances is valid.

There are four different types of fragmentations, which depend on the character of the metal centers, as given by reactions 1–4.

$$Ln^{III}(L)_3^{3+} \rightarrow Ln^{III}(L)_2(L-86)^{2+} + (86)^+ \quad (1)$$

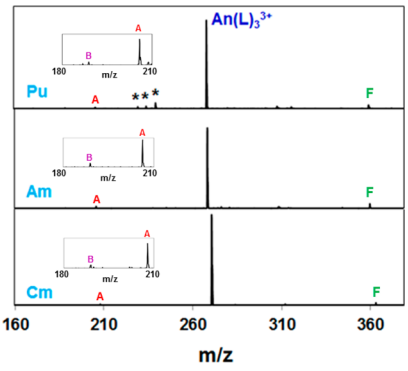

Figure 4. CID mass spectra of $Pu(L)_3^{3+}$, $Am(L)_3^{3+}$, and $Cm(L)_3^{3+}$. Asterisks denote the peaks due to $Pu(L)_2(72)^{3+}$, $Pu(L)_2(86)^{3+}$, and $Pu(L)_2(L{-}86)^{3+}$, in which the oxidation state is Pu(IV). Spectra in the m/z 180–210 region are enlarged in the insets: (A) $An(L)_2^{3+}$; (B) HL^+; (F) $An(L)_2(L{-}86)^{2+}$.

$$Ln^{III}(L)_3^{3+} \rightarrow Ln^{III}(L)(L-H)^{2+} + (HL)^+ \quad (2)$$

$$Ln^{III}(L)_3^{3+} \rightarrow Ln^{III}(L)_2^{3+} + L \quad (3)$$

$$Ln^{III}(L)_3^{3+} \rightarrow Ln^{II}(L)_2^{2+} + (L)^+ \quad (4)$$

$Ln(L)_2(L{-}86)^{2+}$ is a primary CID product for all $Ln(L)_3^{3+}$ complexes (reaction 1), which is characteristic of the fragmentation chemistry of TMOGA coordination complexes, as observed during CID of $AnO_2(L)_2^{2+}$ [6] and $An(L)_3^{4+}$.[10] The $(86)^+$ fragment is presumed to be dehydrogenated *N*,*N*-dimethylacetamide from direct C–O bond cleavage without H or H^+ transfer (Figure 1). This fragmentation by cleavage of a C–O bond in TMOGA is also observed in radiolysis of diglycolamide ligands in aqueous solution.[25] For La, Ce, and Pr, the CID results also revealed formation of HL^+ (reaction 2); this is a very minor product for $Nd(L)_3^{3+}$ and complexes of the later lanthanides. The peak due to $Ln(L)_2^{3+}$ becomes increasingly prevalent for the later lanthanides, particularly for $Lu(L)_3^{3+}$ and $Yb(L)_3^{3+}$ (reaction 3). The appearance of $Ln(L)_2^{3+}$ during CID of late lanthanide–TMOGA complexes suggests that only two TMOGA ligands are required to stabilize a triply charged metal center, at least for the last few members of the lanthanide series. The radii of lanthanides decrease gradually across the series due to the lanthanide contraction, such that it should be decreasingly favorable from La to Lu to accommodate three TMOGA ligands due to steric congestion. For early lanthanides, the neutral ligand loss reaction was not observed; instead, loss of HL^+ to give $Ln(L)(L{-}H)^{2+}$ becomes more favorable; both of these cation products were observed in CID mass spectra of the early Ln.

In the CID spectrum of $Eu(L)_3^{3+}$, $Eu(L)_2^{2+}$ is distinctively the predominant fragmentation product (reaction 4); the peak due to $Eu(L)_2(L{-}86)^{2+}$ is only minor. The dramatic difference in fragmentation behavior between europium and other lanthanides can be rationalized in terms of their reduction potentials: among the Ln(III), Eu(III) is known to be reduced to Eu(II) relatively easily due to its reduction potential of −0.34 V, the lowest in the Ln series.[24] As a result, it is more favorable for Eu(III) complexes to undergo charge reduction concomitant with redox elimination of L^+ than for other lanthanide complexes during CID such that $Eu(L)_2^{2+}$ is the dominant fragmentation product. Note that $Yb(L)_2^{2+}$ is a minor CID product of $Yb(L)_3^{3+}$; the reduction potential of Yb(III), −1.05 V, is lower than that of Eu(III) but higher than that of all other

dx.doi.org/10.1021/ic501985p | Inorg. Chem. 2014, 53, 12135–12140

Ln(III).[24] It has been demonstrated that ligated metal cations tend to undergo reduction if a lower oxidation state is readily accessible.[6,26,27] It is notable that $Ln(L)_2^{2+}$ complexes with a divalent metal center also appeared as minor products during CID of other $Ln(L)_3^{3+}$ complexes. In addition to divalent Eu, Yb, and Sm solid-state complexes, other isolable divalent lanthanide complexes comprising Tm, Dy, and Nd have previously been confirmed by X-ray crystallography.[28,29] These divalent complexes are strong reducing agents due to the much lower reduction potentials of these Ln as compared with Eu, Yb, and Sm.[24,30] Consistent with this notion, the $Nd(L)_2^{2+}$, $Dy(L)_2^{2+}$, and $Tm(L)_2^{2+}$ complexes produced by CID react with residual O_2 in the ion trap to form $Ln(L)_2(O_2)^{2+}$ complexes; in analogy with uranyl superoxides,[21] these oxygen adducts are presumed to be superoxides in which the Ln(II) have been oxidized to Ln(III). Consistent with this interpretation, the divalent Nd, Dy, and Tm complexes add O_2 much more quickly than do $Eu(L)_2^{2+}$, $Yb(L)_2^{2+}$, and $Sm(L)_2^{2+}$ (Figure S4, Supporting Information); no superoxide was observed for $Eu(L)_2^{2+}$ even for a long reaction time of 1 s, in accord Eu(III) having the highest reduction potential among all the lanthanides.[30] Given that the mass of O_2 is the same as that of CH_3OH, an alternative assignment of the $Ln(L)_2(O_2)^{2+}$ peaks would be methanol adducts, $Ln(L)_2(CH_3OH)^{2+}$. However, the distinctive absence of this product for the Ln = Eu complex even after a 1 s reaction period is convincing evidence for oxidation by O_2; a methanol adduct would be produced for all of the complexes, particularly upon application of a long reaction time. Also, there is a clear correlation between the rate of addition of O_2 and the Ln(III) reduction potentials—such a variation in efficiency would not be expected for methanol addition. Addition of oxygen to produce superoxides has been demonstrated as facile in this experimental configuration.[21] Furthermore, it has been demonstrated that the concentration of the ESI solvent in our ion trap is insufficient to form association products. For example, $[UO_2(DAA)_2]^{2+}$ (DAA = diacetone alcohol) complexes prepared by ESI from >99% acetone solutions readily add isopropanol injected into the ion trap, with no evidence for addition of the stronger Lewis base acetone.[31] Another example is addition of acetone to $[UO_2(acetone)_4]^{2+}$ produced by ESI from acetone solution, which occurs only when acetone gas is directly injected into the ion trap.[32] As shown in Figure S4, Supporting Information, other $Ln(L)_2^{2+}$ complexes were produced upon CID (Ln = La, Pr, Gd, Tb). Oxygen addition to these complexes was as facile as for $Nd(L)_2^{2+}$, $Dy(L)_2^{2+}$, and $Tm(L)_2^{2+}$, indicating a comparably strong reducing ability for most divalent lanthanides under these conditions. The correlation between gas-phase CID behaviors of trivalent lanthanide complexes and their condensed-phase reduction potentials is consistent with previous results where gas-phase metal reduction potentials of hydrated metal ions were also found to strongly correlate with the solution reduction potentials.[33−35]

CID of $Am(L)_3^{3+}$ and $Cm(L)_3^{3+}$ mainly resulted in formation of $An(L)_2(L{-}86)^{2+}$ and $An(L)_2^{3+}$ (Figure 4). For $Pu(L)_3^{3+}$, both $Pu(L)_2(L{-}86)^{2+}$ and $Pu(L)_2^{3+}$ were also observed. In addition, three peaks at m/z 229.9, 234.6, and 239.9 appeared during CID of $Pu(L)_3^{3+}$. On the basis of the separation between isotopomer peaks, they are assigned as $Pu(L)_2(72)^{3+}$, $Pu(L)_2(86)^{3+}$, and $Pu(L)_2(L{-}86)^{3+}$, respectively, where the ligands designated as (72), (86), and (L−86) are radical fragments from TMOGA; the (86) and (L−86) fragments result from C−O bond cleavage as indicated in Figure 1, whereas the (72) fragment results from C−C bond cleavage. Since all of these ligands have unpaired electrons that can form chemical bonds to the plutonium center, the oxidation state in these complexes is assigned as Pu(IV); although the structures of the fragments are unknown it is certain that they are radicals with one unpaired electron. Formation of tetravalent species for Pu, but not for Am and Cm, is consistent with the much lower reduction potential for Pu(IV)/Pu(III) (0.98 V) compared with those of Am(IV) (2.3 V) and Cm(IV) (3.1 V).[24] Since $An(L)_2^{3+}$ and $An(L)_2(L{-}86)^{2+}$ are the major fragmentation products during CID of $Pu(L)_3^{3+}$, $Am(L)_3^{3+}$, and $Cm(L)_3^{3+}$ and negligible HL^+ was observed, under CID conditions the three actinide−TMOGA complexes appear to behave similarly to late lanthanide−TMOGA complexes, such as $Yb(L)_3^{3+}$ and $Lu(L)_3^{3+}$.

ETD of $Ln(L)_3^{3+}$, $Pu(L)_3^{3+}$, $Am(L)_3^{3+}$, and $Cm(L)_3^{3+}$. Since all lanthanide trications as well as Pu^{3+}, Am^{3+}, and Cm^{3+} can be stabilized in the gas phase upon coordination by TMOGA, it is possible to probe the gas-phase chemistry of $Ln(L)_3^{3+}$, $Pu(L)_3^{3+}$, $Am(L)_3^{3+}$, and $Cm(L)_3^{3+}$ by ETD. The ETD experiments were performed for the three $An(L)_3^{3+}$ complexes and eight $Ln(L)_3^{3+}$ complexes, with the resulting spectra shown in Figure 5. Recently, ETD has been employed to investigate

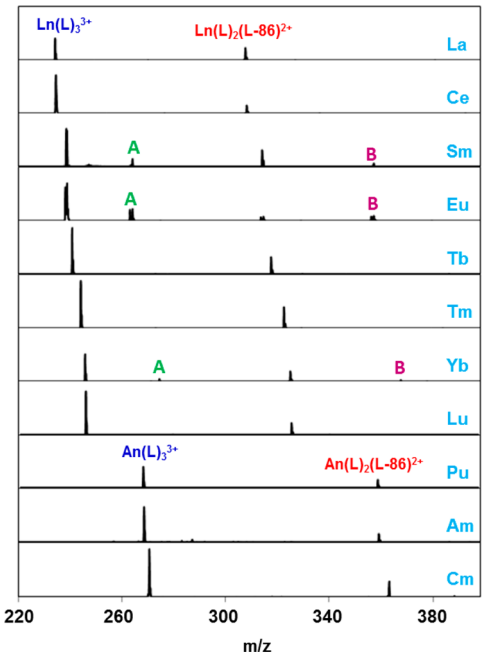

Figure 5. ETD mass spectra of selected $Ln(L)_3^{3+}$, $Pu(L)_3^{3+}$, $Am(L)_3^{3+}$, and $Cm(L)_3^{3+}$: (A) $Ln^{II}(L)_2^{2+}$; (B) $Ln^{II}(L)_3^{2+}$. For those Ln having multiple abundant naturally occurring isotopes, Sm and Yb in these spectra, a single $Ln(L)_3^{3+}$ isotopomer was mass selected for ETD.

the fragmentation and reduction chemistry of solvated uranyl and plutonyl dications as well as TMOGA-stabilized tetrapositive actinide ions.[10,18]

On the basis of fragmentation patterns, the ETD spectra of $Ln(L)_3^{3+}$ can be divided into two groups. The first group is comprised of $Sm(L)_3^{3+}$, $Eu(L)_3^{3+}$, and $Yb(L)_3^{3+}$, where $Ln(L)_2(L{-}86)^{2+}$ as well as the charge reduction products, $Ln(L)_2^{2+}$ and $Ln(L)_3^{2+}$, are the major ETD products (reactions 5−7). For the remaining lanthanide−TMOGA complexes, only $Ln(L)_2(L{-}86)^{2+}$ is observed during ETD (reaction 5). In

dx.doi.org/10.1021/ic501985p | Inorg. Chem. 2014, 53, 12135−12140

reaction 5, a TMOGA ligand fragments via C−O bond cleavage concomitant with charge reduction such that the Ln(III) oxidation state is retained. Since one electron is transferred from $C_{16}H_{10}^{-}$ to $Ln(L)_3^{3+}$ during ETD, the resulting fragmentation products should correlate with the propensity for reduction of Ln(III) to Ln(II). Eu, Yb, and Sm are the three metals in the lanthanide series with the lowest Ln(III)/Ln(II) reduction potentials.[24] Accordingly, charge reduction without ligand fragmentation (reactions 6 and 7) is more favorable for these three complexes than for the others. The ETD results (Figure 5) suggest that reactions 6, 7 (reduction to Ln(II)), and 5 (retention of Ln(III)) are competitive for the Eu, Sm, and Yb complexes. Since the II oxidation state is much less stable for other lanthanides, reaction 5 is dominant. It can be presumed that a transient high-energy $Ln(L)_3^{2+}$ intermediate is formed during the initial electron transfer process; the subsequent intramolecular redox reaction involving cleavage of the C−O bond of TMOGA results in formation of (86) and $Ln(L)_2(L-86)^{2+}$ in which the Ln(III) oxidation state is retrieved. The competition between metal charge reduction and ligand fragmentation has been observed during electron capture dissociation of trivalent lanthanide−peptide complexes.[36]

$$Ln^{III}(L)_3^{3+} + C_{16}H_{10}^{-} \rightarrow Ln^{III}(L)_2(L-86)^{2+} + (86) + C_{16}H_{10} \quad (5)$$

$$Ln^{III}(L)_3^{3+} + C_{16}H_{10}^{-} \rightarrow Ln^{II}(L)_2^{2+} + L + C_{16}H_{10} \quad (6)$$

$$Ln^{III}(L)_3^{3+} + C_{16}H_{10}^{-} \rightarrow Ln^{II}(L)_3^{2+} + C_{16}H_{10} \quad (7)$$

Both $Ln(L)_2^{2+}$ and $Ln(L)_3^{2+}$ were observed during ETD of $Sm(L)_3^{3+}$, $Eu(L)_3^{3+}$, and $Yb(L)_3^{3+}$. Upon the decrease of the charge on the metal centers from the trication to dication, the interaction between the ligands and the metal center decreases, with the result that a ligand can be eliminated. This contrasts with ETD of $Np(L)_3^{4+}$ and $Pu(L)_3^{4+}$, where all three ligands are retained and only the intact reduced charge cations, $Np(L)_3^{3+}$ and $Pu(L)_3^{3+}$, were observed.[10] Observation of $Ln(L)_2^{2+}$ in the gas phase indicates that only two TMOGA ligands are necessary to stabilize the dications. Our previous studies have also shown that trications can be stabilized by only two TMOGA ligands.[10]

ETD of $Pu(L)_3^{3+}$, $Am(L)_3^{3+}$, and $Cm(L)_3^{3+}$ gave rise to simple spectra with only $Pu(L)_2(L-86)^{2+}$, $Am(L)_2(L-86)^{2+}$, and $Cm(L)_2(L-86)^{2+}$, similar to the results for most of the lanthanide−TMOGA complexes. The absence of divalent products during ETD of the actinide−TMOGA complexes is due to the highly unstable character of Pu(II), Am(II), and Cm(II). Unlike these middle actinides, late actinides such as No and Md are believed to have stable II oxidation states;[22] it should be possible to observe $No(L)_2^{2+}$ and $Md(L)_2^{2+}$ upon ETD of $No(L)_3^{3+}$ and $Md(L)_3^{3+}$.

CONCLUSIONS

ESI of mixtures of Ln^{3+} and An^{3+} (Ln = La−Lu, An = Pu, Am, Cm) and TMOGA in methanol resulted in stabilization of gas-phase lanthanide and actinide trications in the form of $Ln(L)_3^{3+}$ and $An(L)_3^{3+}$, analogous to solution species formed during actinide partitioning using diglycolamide ligands. CID and ETD were employed to investigate the stability and fragmentation chemistry of the ligated trications. For the $Ln(L)_3^{3+}$ complexes, both CID and ETD revealed a strong dependence on the nature of the lanthanides. In addition to the common $Ln(L)_2(L-86)^{2+}$ product resulting from $C-O_{ether}$ bond cleavage of TMOGA, early $Ln(L)_3^{3+}$ complexes such as La, Ce, and Pr form the protonated TMOGA cation (HL^+) and $Ln(L)(L-H)^{2+}$ while neutral ligand loss to give $Ln(L)_2^{3+}$ becomes increasingly significant for middle and late lanthanide $Ln(L)_3^{3+}$ complexes. ETD of $Ln(L)_3^{3+}$ parallels the behavior of lanthanide trications in solution. For Sm, Eu, and Yb, which have stable II oxidation states, charge reduction to form $Ln(L)_2^{2+}$ and $Ln(L)_3^{2+}$ as well as $C-O_{ether}$ bond cleavage to form trivalent $Ln(L)_2(L-86)^{2+}$ were observed. For the rest of lanthanides which do not typically exhibit stable II oxidation states, $C-O_{ether}$ bond cleavage to retain the Ln(III) oxidation state was the only fragmentation channel observed during ETD. Since none of the three studied actinides, Pu, Am, and Cm, has a readily accessible II oxidation state, the ETD behavior of the $An(L)_3^{3+}$ complexes is essentially the same as that of $Ln(L)_3^{3+}$ complexes in which the trivalent oxidation state is retained and contrasts with the ETD behavior of $Sm(L)_3^{3+}$, $Eu(L)_3^{3+}$, and $Yb(L)_3^{3+}$. CID of $Pu(L)_3^{3+}$, $Am(L)_3^{3+}$, and $Cm(L)_3^{3+}$ resulted in similar fragmentation patterns to those observed for late lanthanide−TMOGA complexes, such as $Yb(L)_3^{3+}$ and $Lu(L)_3^{3+}$, which suggests that the M^{3+} ionic radii alone do not govern the fragmentation properties. Plutonium exhibited distinctive behavior upon CID whereby Pu(IV) species were produced from $Pu(L)_3^{3+}$. CID clearly reveals the propensity of Pu(III) to oxidized to Pu(IV), as is also the case in solution.

ASSOCIATED CONTENT

Supporting Information

ESI instrumental parameters, ESI and CID mass spectra of the other $Ln(L)_3^{3+}$ and $An(L)_3^{3+}$ complexes, spectra showing reactions of $Ln(L)_2^{2+}$ and O_2. This material is available free of charge via the Internet at http://pubs.acs.org.

AUTHOR INFORMATION

Corresponding Author

*E-mail: jkgibson@lbl.gov.

Notes

The authors declare no competing financial interest.

ACKNOWLEDGMENTS

This work was supported by the U.S. Department of Energy, Office of Basic Energy Sciences, Heavy Element Chemistry, at LBNL under Contract No. DE-AC02-05CH11231.

REFERENCES

(1) Sasaki, Y.; Sugo, Y.; Suzuki, S.; Tachimori, S. *Solvent Extr. Ion Exch.* **2001**, *19*, 91−103.
(2) Ansari, S. A.; Pathak, P.; Mohapatra, P. K.; Manchanda, V. K. *Chem. Rev.* **2012**, *112*, 1751−1772.
(3) Kannan, S.; Moody, M. A.; Barnes, C. L.; Duval, P. B. *Inorg. Chem.* **2008**, *47*, 4691−4695.
(4) Matloka, K.; Gelis, A.; Regalbuto, M.; Vandegrift, G.; Scott, M. J. *Dalton Trans.* **2005**, 3719−3721.
(5) Shkrob, I. A.; Marin, T. W.; Bell, J. R.; Luo, H. M.; Dai, S.; Hatcher, J. L.; Rimmer, R. D.; Wishart, J. F. *J. Phys. Chem. B* **2012**, *116*, 2234−2243.
(6) Gong, Y.; Hu, H. S.; Rao, L. F.; Li, J.; Gibson, J. K. *J. Phys. Chem. A* **2013**, *117*, 10544−10550.
(7) Schröder, D.; Schwarz, H. *J. Phys. Chem. A* **1999**, *103*, 7385−7394.
(8) Schröder, D. *Angew. Chem., Int. Ed.* **2004**, *43*, 1329−1331.
(9) Gong, Y.; Hu, H. S.; Tian, G. X.; Rao, L. F.; Li, J.; Gibson, J. K. *Angew. Chem., Int. Ed.* **2013**, *52*, 6885−6888.

(10) Gong, Y.; Tian, G.; Rao, L.; Gibson, J. K. *J. Phys. Chem. A* **2014**, *118*, 2749−2755.
(11) Blades, A. T.; Jayaweera, P.; Ikonomou, M. G.; Kebarle, P. *Int. J. Mass Spectrom. Ion Processes* **1990**, *101*, 325−336.
(12) Shvartsburg, A. A. *Chem. Phys. Lett.* **2002**, *360*, 479−486.
(13) Shvartsburg, A. A. *J. Am. Chem. Soc.* **2002**, *124*, 7910−7911.
(14) Shvartsburg, A. A. *J. Am. Chem. Soc.* **2002**, *124*, 12343−12351.
(15) Walker, N. R.; Wright, R. R.; Stace, A. J.; Woodward, C. A. *Int. J. Mass. Spectrom.* **1999**, *188*, 113−119.
(16) Puskar, L.; Tomlins, K.; Duncombe, B.; Cox, H.; Stace, A. J. *J. Am. Chem. Soc.* **2005**, *127*, 7559−7569.
(17) Shi, T. J.; Hopkinson, A. C.; Siu, K. W. M. *Chem.—Eur. J.* **2007**, *13*, 1142−1151.
(18) Rios, D.; Rutkowski, P. X.; Shuh, D. K.; Bray, T. H.; Gibson, J. K.; Van Stipdonk, M. J. *J. Mass Spectrom.* **2011**, *46*, 1247−1254.
(19) Gronert, S. *J. Am. Soc. Mass Spectrom.* **1998**, *9*, 845−848.
(20) Rutkowski, P. X.; Michelini, M. C.; Bray, T. H.; Russo, N.; Marçalo, J.; Gibson, J. K. *Theor. Chem. Acc.* **2011**, *129*, 575−592.
(21) Rios, D.; Michelini, M. C.; Lucena, A. F.; Marçalo, J.; Bray, T. H.; Gibson, J. K. *Inorg. Chem.* **2012**, *51*, 6603−6614.
(22) Edelstein, N. M.; Fuger, J.; Katz, J. J.; Morss, L. R. In *The Chemistry of the Actinide and Transactinide Elements*; Morss, L. R., Edelstein, N. M., Fuger, J., Eds.; Springer: Dordrecht, The Netherlands, 2006; Vol. 3, pp 1753−1835.
(23) Mikulas, T.; Chen, M.; Dixon, D. A.; Peterson, K. A.; Gong, Y.; Andrews, L. *Inorg. Chem.* **2014**, *53*, 446−456.
(24) Cotton, S. *Lanthanide and Actinide Chemistry*; Wiley: West Sussex, U.K., 2006.
(25) Sugo, Y.; Sasaki, Y.; Tachimori, S. *Radiochim. Acta* **2002**, *90*, 161−165.
(26) Shvartsburg, A. A.; Wilkes, J. G. *J. Phys. Chem. A* **2002**, *106*, 4543−4551.
(27) Rutkowski, P. X.; Rios, D.; Gibson, J. K.; Van Stipdonk, M. J. *J. Am. Soc. Mass Spectrom.* **2011**, *22*, 2042−2048.
(28) Evans, W. J. *J. Organomet. Chem.* **2002**, *652*, 61−68.
(29) Szostak, M.; Procter, D. J. *Angew. Chem., Int. Ed.* **2012**, *51*, 9238−9256.
(30) Morss, L. R. *Chem. Rev.* **1976**, *76*, 827−841.
(31) Rios, D.; Gibson, J. K. *Eur. J. Inorg. Chem.* **2012**, 1054−1060.
(32) Rios, D.; Schoendorff, G.; Van Stipdonk, M. J.; Gordon, M. S.; WIndus, T. L.; Gibson, J. K.; de Jong, W. A. *Inorg. Chem.* **2012**, *51*, 12768−12775.
(33) Donald, W. A.; Demireva, M.; Leib, R. D.; Aiken, J.; Williams, E. R. *J. Am. Chem. Soc.* **2010**, *132*, 4633−4640.
(34) Donald, W. A.; Leib, R. D.; Demireva, M.; O'Brien, J. T.; Prell, J. S.; Williams, E. R. *J. Am. Chem. Soc.* **2009**, *131*, 13328−13337.
(35) Donald, W. A.; Williams, E. R. *Pure Appl. Chem.* **2011**, *83*, 2129−2151.
(36) Flick, T. G.; Donald, W. A.; Williams, E. R. *J. Am. Soc. Mass Spectrom.* **2013**, *24*, 193−201.